Research article

JHEP|Reports

Molecular clones of genetically distinct hepatitis B virus genotypes reveal distinct host and drug treatment responses

Yongzhen Liu,[1] Debby Park,[1] Thomas R. Cafiero,[1] Yaron Bram,[2] Vasuretha Chandar,[2] Anna Tseng,[3,4] Hans P. Gertje,[3] Nicholas A. Crossland,[3,4] Lishan Su,[5] Robert E. Schwartz,[2,6] Alexander Ploss[1,*]

[1]*Department of Molecular Biology, Lewis Thomas Laboratory, Princeton University, Princeton, NJ, USA;* [2]*Division of Gastroenterology and Hepatology, Department of Medicine, Weill Cornell Medicine, New York, NY, USA;* [3]*National Emerging Infectious Diseases Laboratories, Boston University, Boston, MA, USA;* [4]*Department of Pathology and Laboratory Medicine, Boston University School of Medicine, Boston, MA, USA;* [5]*Division of Virology, Pathogenesis and Cancer, Institute of Human Virology, Department of Pharmacology, University of Maryland School of Medicine, Baltimore, MD, USA;* [6]*Department of Physiology, Biophysics, and Systems Biology, Weill Cornell Medicine, New York, NY, USA*

JHEP Reports **2022.** https://doi.org/10.1016/j.jhepr.2022.100535

Background & Aims: HBV exhibits wide genetic diversity with at least 9 genotypes (GTs), which differ in terms of prevalence, geographic distribution, natural history, disease progression, and treatment outcome. However, differences in HBV replicative capacity, gene expression, and infective capability across different GTs remain incompletely understood. Herein, we aimed to study these crucial aspects using newly constructed infectious clones covering the major HBV GTs.
Methods: The replicative capacity of infectious clones covering HBV GTs A-E was analyzed in cell lines, primary hepatocytes and humanized mice. Host responses and histopathology induced by the different HBV GTs were characterized in hydrodynamically injected mice. Differences in treatment responses to entecavir and various HBV capsid inhibitors were also quantified across the different genetically defined GTs.
Results: Patient-derived HBV infectious clones replicated robustly both *in vitro* and *in vivo*. GTs A and D induce more pronounced intrahepatic and proinflammatory cytokine responses which correlated with faster viral clearance. Notably, all 5 HBV clones robustly produced viral particles following transfection into HepG2 cells, and these particles were infectious in HepG2-NTCP cells, primary human hepatocytes and human chimeric mice. Notably, GT D virus exhibited higher infectivity than GTs A, B, C and E *in vitro*, although it was comparable to GT A and B in the human liver chimeric mice *in vivo*. HBV capsid inhibitors were more readily capable of suppressing HBV GTs A, B, D and E than C.
Conclusions: The infectious clones described here have broad utility as genetic tools that can mechanistically dissect intergenotypic differences in antiviral immunity and pathogenesis and aid in HBV drug development and screening.
Lay summary: The hepatitis B virus (HBV) is a major contributor to human morbidity and mortality. HBV can be categorized into a number of genotypes, based on their specific genetic make-up, of which 9 are well known. We isolated and cloned the genomes of 5 of these genotypes and used them to create valuable tools for future research on this clinically important virus.

Introduction

Chronic HBV infection (CHB) remains a major public health concern affecting at least 296 million patients globally.[4] Patients with CHB are at elevated risk of developing end-stage liver disease, including decompensated cirrhosis and hepatocellular carcinoma (HCC) which accounts for an estimated 820,000 deaths annually.[1] HBV belongs to the *Hepadnaviridae* family with a partially double-stranded, relaxed circular DNA genome of about 3,200 base pairs. HBV has a remarkable genetic plasticity fueled by an error-prone reverse transcriptase/polymerase (error rate of 10^{-4} to 10^{-5}) and high replicative fitness.[2] In chronically infected patients, an estimated 10^{12} viral particles are generated daily. This results in tremendous genetic diversity, translating into readily acquired viral resistance or escape from immune pressure. HBV has been phylogenetically classified into 9 genotypes (GTs) A-I with an intergenotypic divergence of greater than 7.5%.[3,4] An additional HBV strain, isolated from a Japanese patient in 2009 was provisionally assigned as a putative 10th GT 'J',[5] but it has not yet been recognized as an independent GT.[6] GTs are further divided into sub-GTs when the nucleotide heterogeneity across the genome exceeds 4%, highlighting the remarkable heterogeneity of HBV.[3,4]

HBV GTs have different geographic distributions and are associated with ethno-geographic ranges, population migration and HBV evolution.[7,8] Based on publicly available HBV genotyping data, GTs A and D were broadly distributed and predominant across Europe, Western and Central Asia, North and South Africa, and North and Central America.[9] In Eastern and Southeastern Asia, and Australasia, GTs B and C are more prevalent, while GTs E and F are commonly found in sub-Saharan African and Latin

Keywords: hepatitis B virus; hepatitis B; viral hepatitis; genotypes; reverse genetics; host responses; drug development.
Received 9 May 2022; received in revised form 27 June 2022; accepted 4 July 2022; available online 9 July 2022
* Corresponding author. Address: Department of Molecular Biology, Lewis Thomas Laboratory, Princeton University, Princeton, NJ, USA; Tel.: +1 (609)-258-7128.
E-mail address: aploss@princeton.edu (A. Ploss).

American countries, respectively[10–12] (Fig. S1). Notably, GTs A to E account for about 96.2% of all chronic HBV infections globally.[9]

Progression and development of CHB to severe liver disease is usually determined by the host genetic background as well as by environmental factors and HBV viral factors. Different HBV GTs have been linked to differences in pathogenesis, disease progression and responses to antiviral therapy.[12,13] A clinical study showed that GT A appears to have a higher propensity for chronic infection than GTs B or C.[14] Other case-controlled studies suggest that infections with GT C result in exacerbated pathogenesis including a higher risk of developing HCC than GT B.[15–17] Patients infected with GT C HBV were also reported to have higher HBV DNA load, delayed HBeAg seroconversion,[18] lower interleukin (IL)-21 levels and lower numbers of HBV-specific cytotoxic T lymphocytes.[19] Different HBV GTs also exhibit different sensitivities to antiviral therapy. Patients infected with GTs A or B are more likely to achieve a sustained virologic response (SVR) when treated with interferon-α (IFN-α)-based therapy compared with those infected with GTs C and D.[20–22] The response to nucleos(t)ide analogue (NA) treatment across HBV GTs appears to be similar[20,23] but development of drug resistance may vary among different GTs.[24] These examples highlight the importance of intergenotypic differences between HBV GTs which ought to be more extensively taken into consideration.

The lack of genetically defined infectious clones for the 5 major GTs A-E has largely precluded the direct comparison of their virological characteristics, such as viral replication, antigen expression, and specific functional elements. Plasmids encoding 1.24-mer[25] or 1.28-mer[26] HBV genomes have previous been transfected into Huh7 cells, to compare viral replication and antigen expression phenotypes of GTs A to D, but only the infectivity of GT A and C were investigated. Comparing HBV replication and protein expression among GTs A-D and the minor or putative gt J suggested that GTs B, C and J appear to replicate less efficiently than GT D.[27] While these data are intriguing, HBV infectivity assays across the different GTs were not included. Previously, patient-derived HBV genome clones were constructed for GTs B and C, and their infectivity with or without a preS1 N-terminal deletion was investigated.[28] However, these HBV virions (HBVcc) were produced in cell culture from 1.1-mer HBV constructs in which HBV replication was driven by the ectopic strong cytomegalovirus (CMV) promoter rather than endogenous HBV promoters. Murayama *et al.* directly compared the infectivity of virions harvested from cell culture supernatants following transfection of 1.38-mer HBV genome of GTs C and D and found GT D virus caused more robust infection in HBV-permissive HepG2-hNTCP hepatoma cells due to a deletion in the preS1 N-terminal domain.[29] More recently, Zhang *et al.* tested the infectivity of GTs A, B, C, D, E, F and H and their responsiveness to IFN-α treatment, by using HBV virions from selected HBV-producing stable cell lines, respectively.[30] However, generating stable cell lines for different GTs is time-

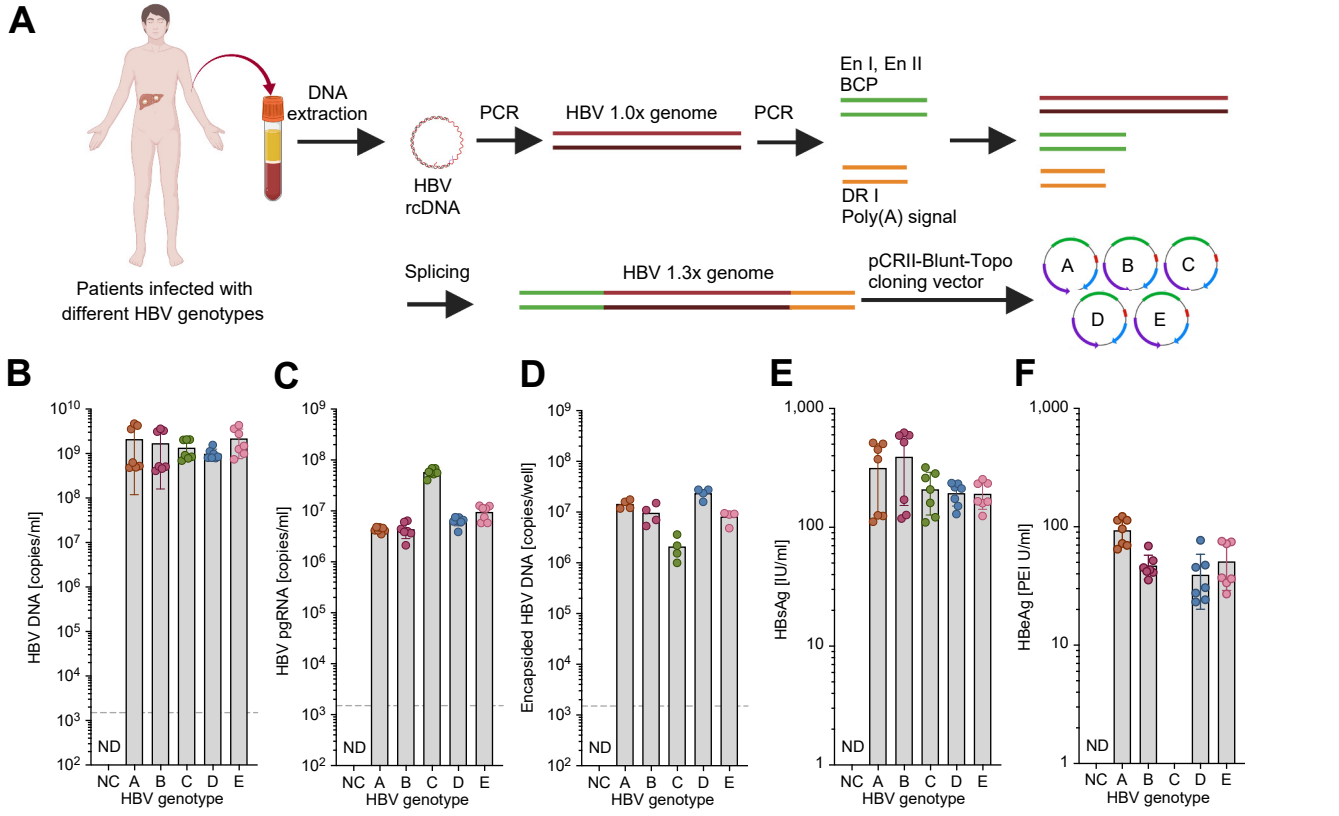

Fig. 1. Construction and characterization of 1.3-mer HBV infectious clones of genotypes A to E. (A) Schematic workflow for the generation of the HBV 1.3-mer infectious clones of genotypes A-E. Quantification of HBV DNA (B) and pgRNA (C) copy numbers by qPCR and RT-qPCR, respectively. (D) Encapsidated HBV DNA inside of the cells was extracted and quantified by qPCR. Quantification of HBsAg (E) and HBeAg (F) by CLIA in cell culture supernatants 48 hours post transfection of HBV genotype clones. Limit of detection for the qPCR assay ≈10^3 copies/ml or 10^3 copies/well. Data shown as mean ± SD and at least 4 independent experiments were performed for each genotype. BCP, basic core promoter; DR, direct repeat; En, enhancer; NC, negative control; ND, not detected; pgRNA, pregenomic RNA; rcDNA, relaxed circular DNA.

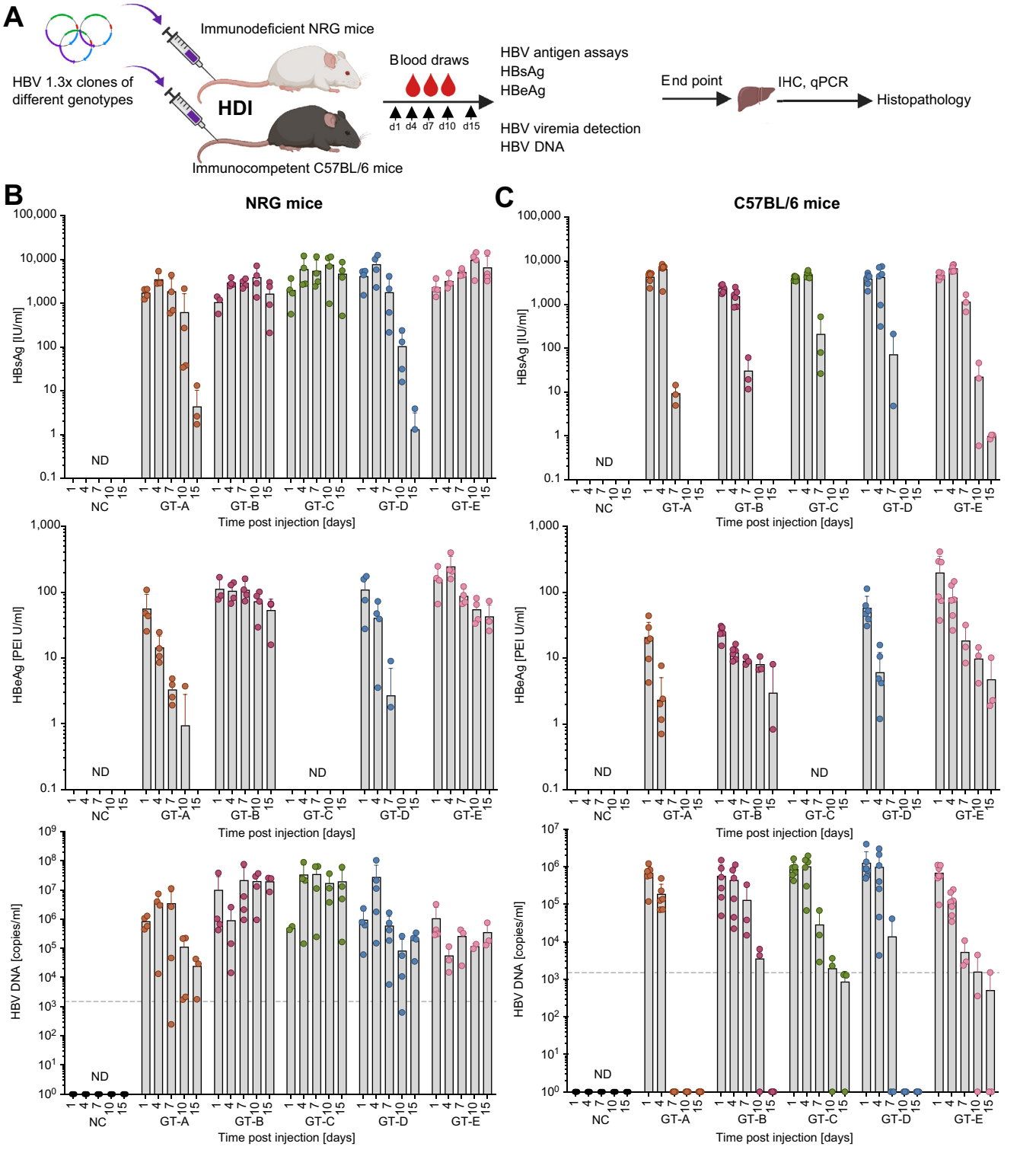

Fig. 2. HBV 1.3-mer infectious clones of different genotypes replicate robustly *in vivo*. (A) Schematic of experimental procedures. (B) Longitudinal HBsAg (up), HBeAg levels (middle) and HBV DNA (bottom) of different HBV genotypes in NRG mice (n = 4) through 1 to 15 days after the plasmid delivery. (C) Longitudinal HBsAg (up), HBeAg levels (middle) and HBV DNA (bottom) of different HBV genotypes in C57BL/6 mice (start point n = 6, euthanized 3 mice at day 5) through 1 to 15 days after plasmid delivery. Limit of detection of the detection systems for HBV DNA $\approx 10^3$ copies/ml. Data shown as mean ± SD. GT, genotype; HDI, hydrodynamic injection; IHC, immunohistochemistry; NC, negative control; ND, not detected; NRG, NOD *Rag1*$^{-/-}$ IL2Rγ NULL; qPCR, quantitative PCR.

consuming and single cell-derived cell clones may not be representative of the true virological features of the chosen genome due to differences across the producer cell lines in terms of viral genome copy numbers, integration sites and cellular environment.

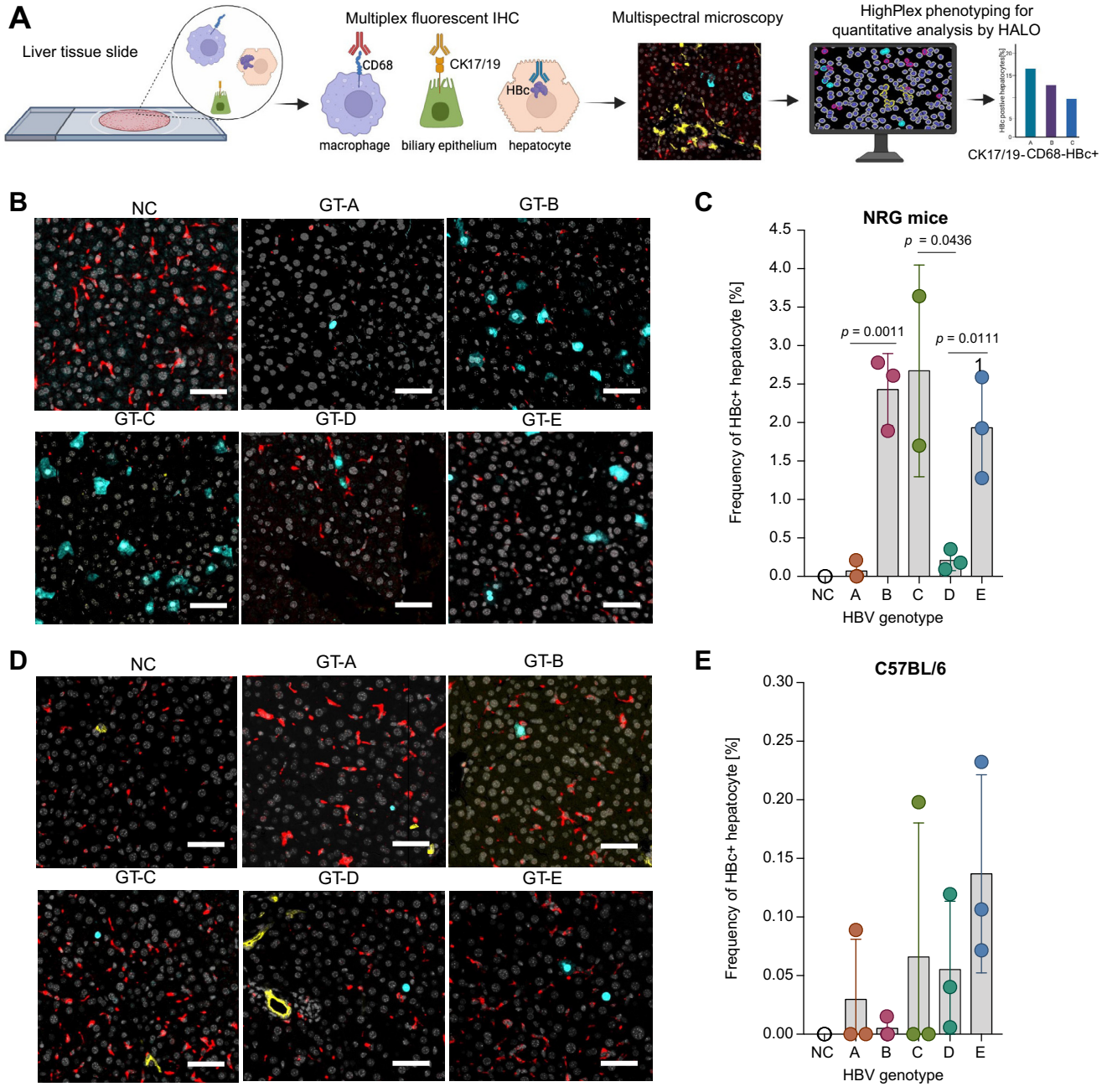

Fig. 3. Quantification of HBc expression in liver tissues in NRG and C57BL/6 mice by multiplex fluorescent IHC. (A) Schematic of the multiplex fluorescent IHC and quantitative analysis. Representative images of multiplex fluorescent IHC of the liver sections 15 days post hydrodynamic tail vein injection of different HBV genotype infectious clones into NRG (B) and C57BL/6 (D) mice (n = 3). HBc-positive signals are shown as cyan, macrophages as red, and biliary epithelium cells (when depicted in the field of view) as yellow. Frequencies of HBV core protein positive in livers of NRG (C) and C57BL/6 (E) mice. Data shown as mean ± SD of 3 mice except genotype C. Unpaired 2-tailed *t* test. The scale bar = 50 μm. GT, genotype; IHC, immunohistochemistry; NC, negative control group mice injected with equal volume of sterile PBS; NRG, NOD *Rag1*$^{-/-}$ IL2RγNULL.

To bridge this technical and knowledge gap we constructed genetically defined infectious clones of HBV GTs A, B, C, D and E. All 1.3x length HBV genomes were replication-competent and produced virions that were infectious in HepG2-hNTCP cell lines, primary human hepatocytes (PHH) and human liver chimeric mice. Hydrodynamic delivery of these genomes into immunocompromised mice resulted in sustained viremia whereas immunocompetent animals cleared the infection within 5-10 days. In immunocompetent animals, HBV GTs A and D were more rapidly cleared than the other GTs, and the lower frequencies of hepatocytes expressing HBcAg correlated with elevated levels of proinflammatory cytokines and more pronounced intrahepatic immune cell infiltration. Further, we established proof-of-concept for the utility of the infectious clones as a tool to dissect viral genetic determinants controlling viral protein expression. Finally, we demonstrated that the infectious clones exhibited distinct sensitivities to HBV capsid inhibitors. Taken together, our data highlight the importance for considering intergenotypic differences when analyzing host and drug

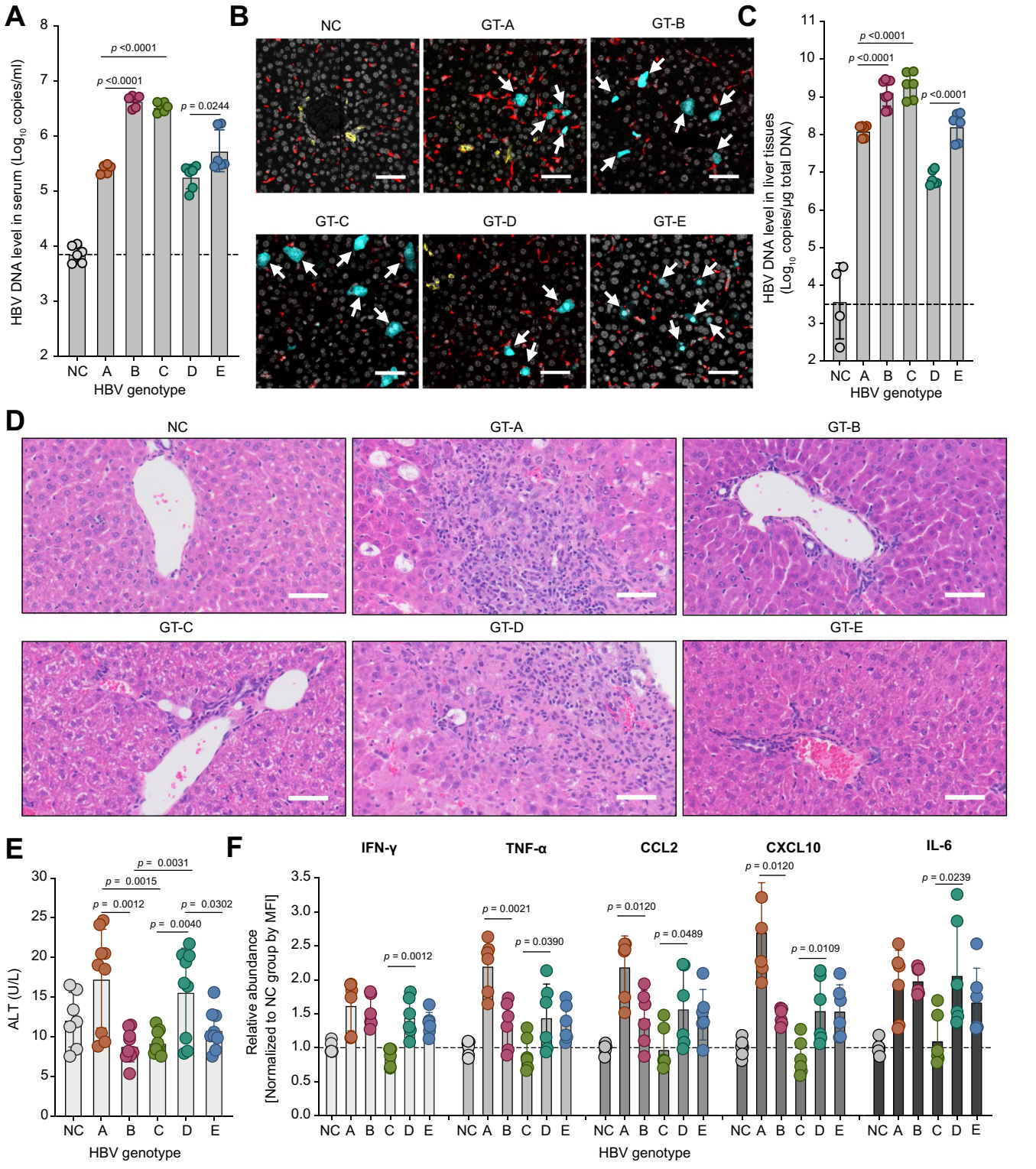

Fig. 4. HBV genotypes A and D cause a more pronounced inflammatory response in C57BL/6 mice. (A) Quantitative assay of HBV DNA in the mouse sera 5 days post HDI. Data shown as mean ± SD of 3 mice and the HBV DNA was determined twice independently. Unpaired 2-tailed *t* test. (B) Representative images and quantitative assay of multiplex fluorescent immunohistochemistry of the liver sections 5 days post hydrodynamic tail vein injection of different HBV genotype infectious clones into C57BL/6 mice (n = 3). HBc-positive signals as indicated by arrowheads were shown as cyan, macrophages as red while biliary epithelium cells (when depicted in the field of view) as yellow. The scale bar was 50 μm. (C) Quantitative assay of HBV DNA in the mouse liver tissues. Data shown as mean ± SD of 3 mice and the HBV DNA was determined twice independently. Unpaired 2-tailed *t* test. (D) Representative images of H&E staining of the liver sections 5 days post hydrodynamic tail vein injection of different HBV genotype infectious clones into C57BL/6 mice (n = 3). (E) ALT levels in mouse sera injected with PBS control or different genotype plasmids, respectively. Data shown as mean ± SD of 3 mice and the test was performed 3 times independently. Unpaired 2-tailed *t* test. (F) Quantification of IFN-γ, TNF-α, CCL2, CXCL10 and IL-6 levels in mouse sera. The expression level was normalized to NC group. Data shown as mean ± SD of 3 mice and the test was performed twice independently. An unpaired 2-tailed *t* test was used to determined statistical significance. NC, negative control group mice injected with equal volume of sterile PBS. ALT, alanine aminotransferase; GT, genotype; MFI, mean fluorescent intensity.

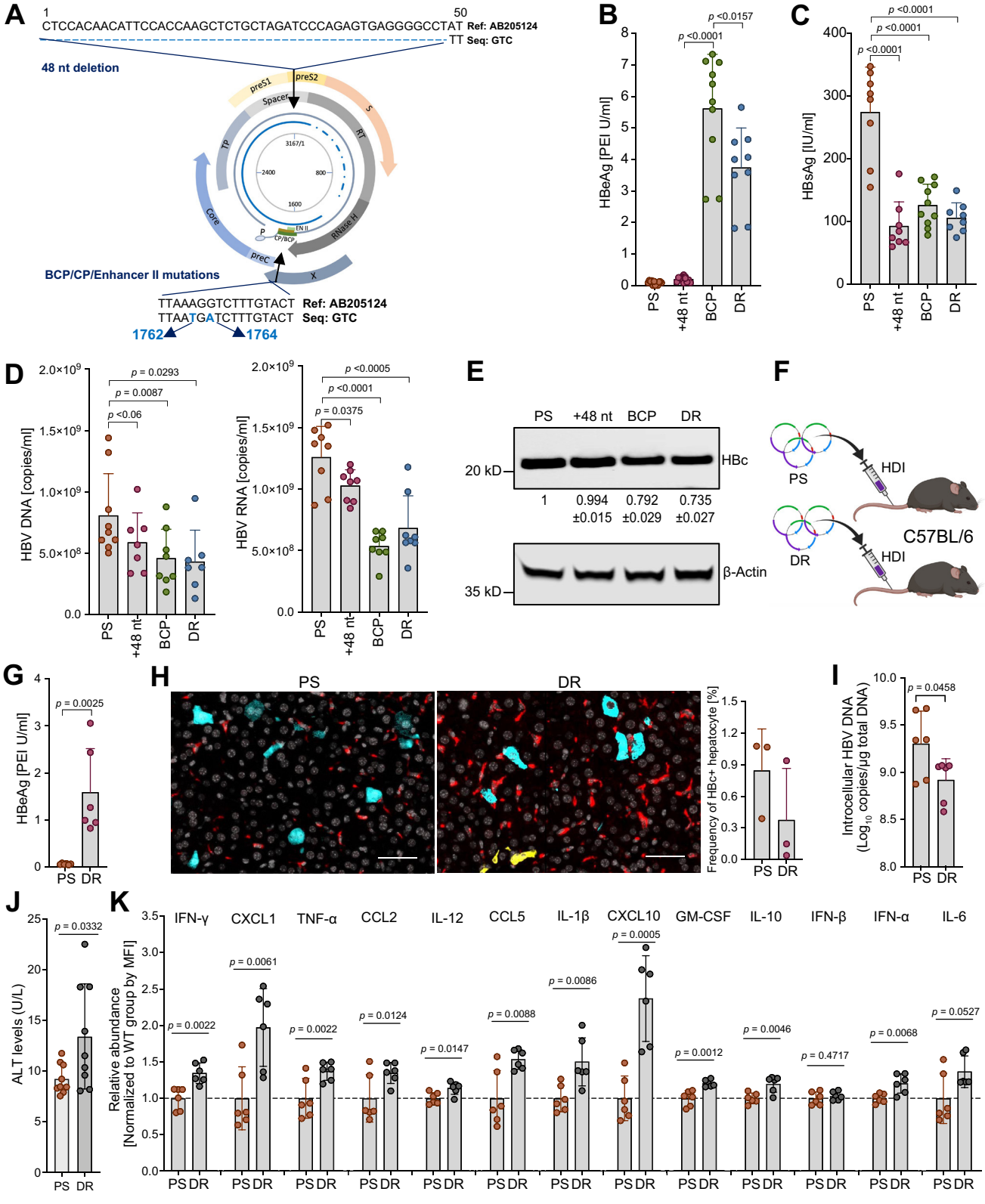

Fig. 5. HBeAg expression contributes to HBV-induced hepatic inflammation in C57BL/6 mice. (A) Schematic diagram showing the GT C strain used in this study has a 48-nt deletion and A1762T, G1764A mutations compared with the GT C sequences in the database (NCBI no. AB205124) in the HBV genome. Quantification of HBeAg (B), HBsAg (C) by CLIA, and HBV DNA and pgRNA (D) by qPCR and RT-qPCR in culture supernatants and HBcAg by western blotting (E) in lysates of cells transfected with HBV GT C genomes in which the different mutations had been corrected or not. Data shown as mean ± SD. Unpaired 2-tailed *t* test. (F) Schematic representation of the workflow for the characterization of the HBV GT mutant infectious clones in C57BL/6 mice. (G) HBeAg expression in mouse serum 1 day after the HDI (n = 6). Data shown as mean ± SD. Unpaired 2-tailed *t* test. (H) Representative images of multiplex fluorescent immunohistochemistry and the corresponding quantitative assay of HBV core protein positive hepatocyte percentage against all the hepatocytes of the liver sections 5 days post HDI of

treatment responses, and we provide tools for systematically analyzing such differences.

Materials and methods

A detailed description of the materials and methods used in this study is included in the supplementary information.

Results

Construction and characterization of infectious clones of HBV GTs A-E

To construct HBV replication-competent clones of different GTs, HBV genomes covering HBV GTs A-E were amplified from patient sera or cell culture supernatants (Fig. 1A). Using PCR, we amplified HBV replication modulators, enhancer 1 (En 1), En 2 and basic core promoter (BCP), which are important for HBV reverse transcription initiation and localize at about nucleotide (nt) 960-1825 in the HBV genome. We also amplified direct repeat 1 (DR1) and polyadenylation signal, which regulate HBV RNA production and localize at about (nt) 1820-2000. HBV replication modulators and regions with DR1 and polyadenylation signal were then spliced and added to the 5' and 3' ends of the amplified 1.0x HBV genome and inserted into the same pCRII-Blunt-TOPO vector backbone to generate the 1.3-mer HBV replication-competent clones of HBV GTs A, B, C, D and E, respectively (Fig. 1A). HBV GT identity was further confirmed by sequence alignment with prototypic sequences of the respective GTs (Fig. S2).

To characterize their replicative capacity, these genetically defined clones were transfected into HepG2 human hepatoma cells. All HBV GTs replicated robustly as evidenced by HBV DNA copy numbers exceeding 10^9 copies/ml in the supernatants (Fig. 1B). HBV DNA copy numbers remained at high levels (>10^8 copies/ml) for at least 8 days post transfection (Fig. S3). Since HBV RNA in patient serum or supernatants of HBV cell models has previously been identified as encapsidated pre-genomic RNA (pgRNA) that is associated with HBV replication in the reverse transcription process,[31,32] pgRNA was also quantified by reverse-transcription quantitative PCR (RT-qPCR). pgRNA exceeded 10^6 copies/ml and GT-C pgRNA was about 10-fold higher than other GTs (Fig. 1C) while for intracellular encapsidated HBV DNA, GT-C was about 10-fold lower (Fig. 1D), suggesting that GT-C secreted more premature pgRNA-containing particles in which reverse transcription had not been completed. HBsAg expression was equivalently high across the different GTs (Fig. 1E). While HBeAg was found at similar levels for GTs B, D and E, it was found to be about 2-fold higher for GT A, but not expressed for GT C (Fig. 1F). Collectively, these data demonstrate that the 1.3x HBV genomes are replication-competent *in vitro*.

HBV clones of different GTs can replicate robustly in immunodeficient and immunocompetent mice

To assess the replicative fitness of the different HBV GTs *in vivo*, immunodeficient NOD *Rag1*$^{-/-}$ IL2RγNULL (NRG)[33] and immunocompetent C57BL/6 mice received a hydrodynamic injection (HDI) with endotoxin-free plasmids encoding the 1.3x genomes or the same volume of sterile PBS (as a negative control). Different virologic parameters were quantified on days 1, 4, 7, 10 and 15 after injection (Fig. 2A). In NRG mice, HBsAg (~1,000 IU/ml) and HBeAg (~100 PEI U/ml) were equivalently high across all cohorts 1 day post HDI. Viral antigen levels were sustained for GTs B, C and E over the entire study period but decreased for GTs A and D by 7 days post HDI (Fig. 2B, upper and middle panels). HBV DNA copy numbers ranged from 5x10E+5 - 1x10E+7 across all 5 GTs but declined 2-3 log for GTs A and D thereafter until 15 days post injection (dpi, Fig 2B, bottom). Consistent with previous observations,[34] for C57BL/6 mice, HBsAg concentrations peaked in the sera 1-4 days after injection, declined significantly by day 7 and dropped below the limit of detection by day 10 post HDI except for GT E (Fig 2C, top). HBeAg levels followed overall similar patterns but were more sustained for GTs B and E (Fig 2C, middle). HBV DNA levels declined faster in C57BL/6 mice and the viremia approached or fell below the limit of detection as early as day 7 for GTs A and D after injection while it lasted longer in GTs B, C and E (Fig. 2C, bottom).

We next aimed to quantify any potential differences in the frequencies of HBc-bearing hepatocytes. Thus, we employed a multiplex fluorescent immunohistochemistry approach to mark and exclude HBV non-susceptible macrophages (CD68) and biliary epithelium cells (CK17/19) to specifically investigate the HBc expression in hepatocytes (Fig. 3A). After whole-slide imaging, quantitative analysis was performed automatically through HighPlex phenotyping and phenotypes of either HBc+ or HBc- hepatocytes were determined by selecting inclusion and exclusion parameters as follows: CK17/19-CD68-HBc+ or CK17/19-CD68-HBc- (Fig. 3A). The results showed that our multiplex fluorescent immunohistochemistry system worked well to employ CD68, CK17/19 and HBc antibodies simultaneously for staining macrophages, biliary epithelium cells and HBc-positive hepatocytes (Fig. 3B, D). Quantitative analysis indicated that hydrodynamic delivery of all 5 GTs resulted in HBc protein expression in livers of NRG mice 15 dpi. The frequencies of HBc-positive hepatocytes were 2.428±0.271% for GT B, 2.672±0.973% for GT C, and 1.932±0.678% for GT E, while the frequencies were markedly lower for GTs A and D at 0.072 ± 0.069% and 0.210±0.077%, respectively (Fig. 3C). Expectedly, HBc expression was low in the livers of immunocompetent C57BL/6 mice, presumably due to the clearance of HBV antigen-bearing cells by the ensuing immune response (Fig. 3D, E). Overall, these data are consistent with the serum viremia markers (Fig. 2B, C) and highlight GT-specific differences in the replicative ability of these genomes.

HBV GTs A and D induce a more pronounced inflammatory response in mice compared with GTs B, C and E

Since viral antigen levels decreased quickly for GTs A and D both in NRG mice and C57BL/6 mice (Fig. 2), and the frequencies of HBc-positive hepatocytes were also lower in mice injected with these 2 GTs compared with GTs B, C and E (Fig. 3), we aimed to

parental GT-C strain (PS) or double restoration (DR) GT C infectious clones injected into C57BL/6 mice (n = 3). HBc-positive signals are shown as fluorescent green, macrophages as red, and biliary epithelium cells (when included in the view) as yellow. The scale bar = 50 μm. (I) Intracellular HBV DNA in the liver tissues was detected by qPCR. Data shown as mean ± SD. Unpaired 2-tailed *t* test. (J) ALT levels in the mouse sera injected with parental GT C strain (PS, n = 3) or GT C with double restoration (DR, n = 3). Data shown as mean ± SD of 3 mice and the test was performed 3 times independently. (K) Mouse antiviral response profile between wild-type or double mutant GT C infectious clones in C57BL/6 mice. The expression level was normalized to the parental GT-C strain (PS) group. Data shown as mean ± SD of 3 mice and the test was performed twice independently. An unpaired 2-tailed *t* test was used to determined statistical significance. MFI, mean fluorescent intensity. ALT, alanine aminotransferase; BCP, GT C clone with T1762A and A1764G restoration; DR, GT C clone with both the 48 nt replenishment and T1762A and A1764G replacements; HDI, hydrodynamic injection; PS, parental GT C strain; +48 nt GT C clone with 48 nt replenishment.

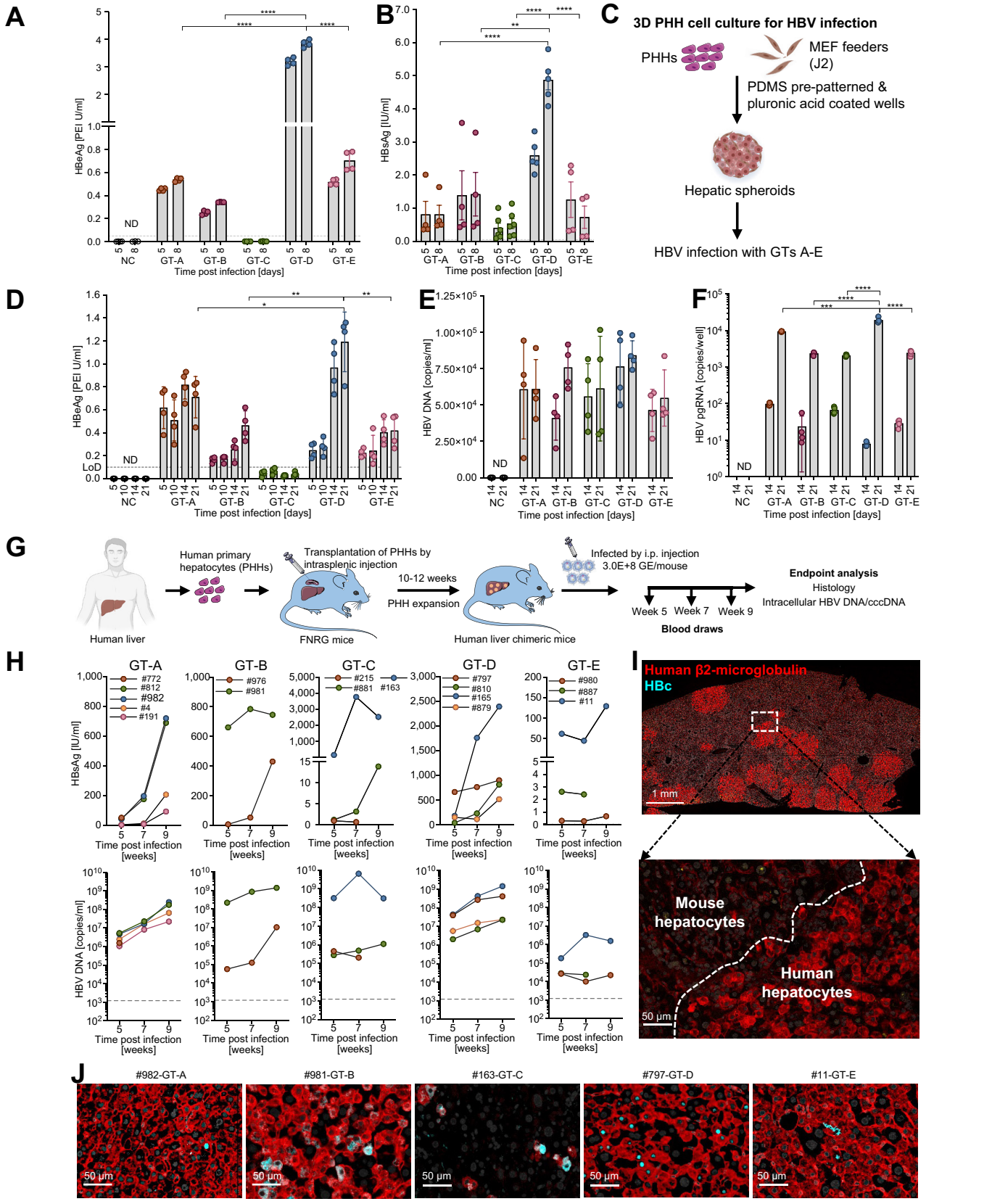

Fig. 6. HBV infectivity of different genotypes *in vitro* and in human hepatocyte chimeric mice. Quantification of HBeAg levels in supernatant of HepG2-hNTCP cells infected with HBV GTs A, B, C, D and E (A) or HBsAg levels (B) at a MOI of 8,000. Naïve HepG2 cells exposed to same amount of GT D virus were used as a negative control (NC). The HBsAg levels were normalized by subtracting the background in NC group. The data are shown as mean±SD of at least 4 independent experiments. Unpaired 2-tailed *t* test. $^{**}p$ <0.01; $^{****}p$ <0.0001. (C) Schematic of HBV infection of PHHs in 3D organoids. (D) HBeAg levels in the supernatants on 5-, 10, 14-, 21-dpi. The data are shown as mean ± SD of 4 independent experiments. Unpaired 2-tailed *t* test. $^{*}p$ <0.05; $^{**}p$ <0.01. HBV DNA (E) and pgRNA detection (F) in the supernatants 14- and 21-dpi by qPCR and RT-qPCR, respectively. PHHs were inoculated at a MOI of 8,000 with the different HBV GTs.

gain more in-depth insights into the mechanism(s) underlying GT-specific viral (antigen) clearance. In C57BL/6 mice 5 days post HDI, HBV DNA and HBeAg levels were lower in circulation (Fig. 4A, Fig. S4) and less hepatocytes were HBcAg+ (Fig. 4B) for GTs A and D when compared with the other GTs. Consistently, intracellular HBV DNA copy numbers were also reduced in the livers of C57BL/6 mice 5 days post HDI with GTs A and D compared to GTs B, C and E (Fig. 4C). At 5 days post HDI, histological analysis of 1 GT A mouse (n = 3) and 2 GT D mice (n = 3) revealed evidence for hepatic fibrosis, mixed inflammation, and hepatocellular microvesicular vacuolation, which is potentially representative of hepatocyte degeneration/dysfunction (Fig. 4D). This was not seen for other GTs. The apparently more pronounced immune-mediated liver damage in GTs A and D was further supported by elevated alanine aminotransferase (ALT) levels, a marker for liver damage, for these genotypes (Fig. 4E). Consistent with more pronounced intrahepatic immune infiltration, the concentrations of multiple proinflammatory cytokines (IFN-γ, TNF-α, IL-6) and chemokines (CCL2 and CXCL10) were higher in sera of immunocompetent C57BL/6 mice injected with GTs A and D compared with the other GTs (Fig. 4F, Fig. S5).

Infectious clones are a versatile tool to dissect viral genetic determinants controlling viral protein expression

To determine the molecular basis for the apparent absence of HBeAg expression in the GT-C clone we selected, its genome was compared with other GT C strains. Notably, 2 major mutations were detected in our patient-derived parental GT C strain (abbreviated PS), namely a 48-nt deletion located at HBV nt 1-48 in the preS2 gene and A1762T and A1764G mutations in the CP, BCP and En II overlapping gene expression regulatory regions (Fig. 5A). To investigate the significance of these mutations, we replenished the +1-48 nt (abbreviated +48 nt), reverted the T1762A A1764G (abbreviated BCP) separately or combined the double restoration mutations (abbreviated DR) in the GT C clone. Although replenishing 1-48 nt did not enhance HBeAg expression, T1762A and A1764G back mutations did significantly increase HBeAg levels (p <0.0001) (Fig. 5B). Combining the T1762A and A1764G reversion with the 1-48 nt insertion had no further additive effect but rather decreased HBeAg levels in transfected cells (p = 0.0157) (Fig. 5B). Since the 1-48 nt deletion is positioned within the preS2 region, we further tested the effects of these restoration mutations on HBsAg expression. Replenishing 1-48 nt and/or the T1762A/A1764G reversion all significantly reduced HBsAg levels (p <0.0001) (Fig. 5C). To gain more insights into how these mutations affected replicative ability compared to the parental GT C strain, we quantified viral replication intermediates and protein expression *in vitro*. Consistent with the reduction in HBsAg expression (Fig. 5C) HBV DNA and pgRNA copy numbers were also reduced in the GT C genomes harboring the individual or combined mutations (Fig. 5D). Similarly, HBcAg expression as assessed by western blotting was also reduced by about 30% in DR *vs.* PS GT C (Fig. 5E).

We next aimed to determine whether restoration of HBeAg expression would affect the replicative ability of the HBV GT C strain *in vivo* in comparison to the isogenic parental genome (Fig. 5F). Consistent with our data in cell culture, the DR rescued HBeAg expression but reduced HBc protein expression following hydrodynamic injection of the mutant and original genomes into C57BL/6 and NRG mice (Fig. 5F-H and Fig. S6). Intracellular HBV DNA in the liver tissues was also lower in mice injected with HBV containing double restoring mutations compared with that of the parental stain group (Fig. 5I). The dynamics of HBsAg, HBeAg and HBV DNA in NRG and C57BL/6 mouse sera on days 1, 4, 7, 10 and 15 post injection for these 2 strains are shown in Fig. S7. Notably, the DR GT C virus induced a more severe liver damage characterized by higher ALT levels (Fig. 5J) and a universally stronger antiviral inflammatory response, as evidenced by higher expression of IFNs and other proinflammatory cytokines and chemokines (Fig. 5K). Taken together our data provide insights into the impact of HBeAg expression on viral replication dynamics and pathogenesis, and establishes proof-of-concept for the utility of the infectious clones for reverse genetics approaches.

Comprehensive comparison of HBV infectivity across GTs *in vitro* and in human hepatocyte chimeric mice

Next, we aimed to determine how efficiently different GTs of HBV establish infection *in vitro* and *in vivo*. We first infected HepG2-NTCP cells (3B10 clone[35]) at a multiplicity of infection (MOI) of either 4,000 or 8,000. At MOI = 8,000, HBeAg concentrations increased longitudinally in culture supernatants (Fig. 6A). The infectivity of GT D was significantly higher than that of GTs A (p <0.0001), B (p <0.0001) and E (p < 0.0001), as characterized by the HBeAg level 8 dpi at either MOI (Fig. 6A and Fig. S8). Expectedly, for the parental HBV GT C strain, HBeAg was not detectable due to the aforementioned mutations (Fig. 5). However, HBsAg secreted from parental HBV GT C-infected cultures, albeit at lower amounts than from HBV GT D-infected cells (p <0.0001) (Fig. 6B).

We further analyzed HBV infection cultures of primary human hepatocytes using a 3D hepatocyte spheroid culture platform that has previously been shown to maintain hepatocyte function and HBV permissiveness long-term.[36] Primary human hepatocytes were inoculated at a MOI of 8,000 with the different HBV GTs (Fig. 6C). HBeAg and HBV DNA concentrations increased longitudinally in culture supernatants (Fig. 6D, E). HBV DNA production in the supernatant was maintained over 21 days. HBV pgRNA was detected in all genotypes and increased over time (Fig. 6F). Consistently, the infectivity of GT D was greater than that of GTs A, B, C, and E based on HBeAg and HBV pgRNA production (Fig. 6D, F)

Finally, the infectivity of different HBV GTs was assessed in human liver chimeric mice. Highly engrafted humanized mice (>1,000 μg/ml of human albumin in circulation, Fig. S9A) were injected intraperitoneally with 3.0E+8 genome equivalents of the different HBV GT virions per mouse (Fig. 6G). HBsAg and HBV DNA increased between weeks 7-9 post-infection in most animals irrespective of the inoculum (Fig. 6H). It should be noted though that infection efficiencies varied and HBsAg and HBV

The data are shown as mean±SD of 4 independent experiments. Unpaired 2-tailed t test. ****p <0.0001. (G) Schematic of the experimental procedures of HBV infection in human liver chimeric mice. (H) HBsAg (up) and HBV DNA (down) were quantified in the sera of human liver chimeric mice at the indicated timepoints. (I) Representative images show the two-plex fluorescent immunohistochemistry including human specific β2-microglobulin and HBc staining. (J) Representative images show the two-plex fluorescent immunohistochemistry in human liver chimeric mice infected with different HBV GTs. HBc-positive signals are shown as cyan, chimeric human hepatocytes in the mouse livers are indicated by human specific β2-microglobulin as red. GT, genotype; NC, negative control; ND, not detected; PHH, primiary human hepatocyte.

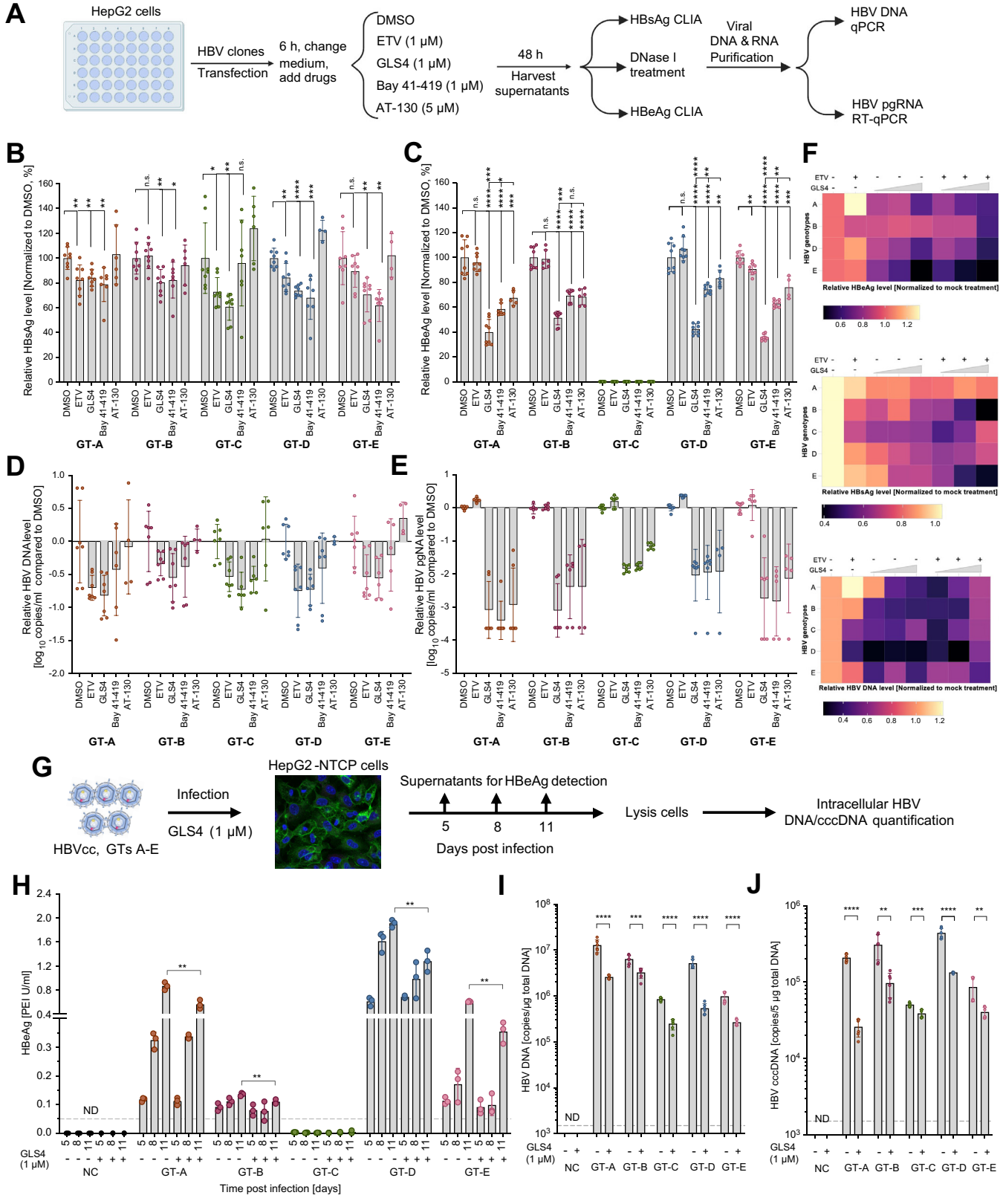

Fig. 7. Differences in treatment responses for different HBV genotypes to different HBV therapeutics. (A) Schematic showing the antiviral treatment and detection makers of HBV different genotypes by clinically (entecavir, ETV) or pre-clinically (type I CpAM GLS4, Bay 41-419 and type II CpAM AT-130) relevant drugs. Quantification of HBsAg (B) and HBeAg (C) by CLIA, HBV DNA (D) and pgRNA (E) by qPCR and RT-qPCR in the supernatants of cells transfected with the 1.3x HBV genomes and following 48 hours of antiviral drug treatment. Data were normalized to the DMSO condition and the original levels were shown in Fig. S12. Data shown as mean ± SD. Unpaired 2-tailed *t* test. (F) Heat maps of HBeAg (up), HBsAg (middle) and HBV DNA (down) levels in the supernatants of cells

DNA levels in the serum were higher for GTs A, B and D than for GT E (Fig. 6H). Correspondingly, a similar trend was observed for intracellular HBV markers including HBV DNA and HBV covalently closed circular DNA (cccDNA) in liver tissues harvested at 9 weeks post HBV infection (Fig. S9B-D). We also investigated the *in situ* HBc expression in the human liver chimeric mouse livers by taking advantage of two-plex fluorescent immunohistochemistry including human specific β2-microglobulin and HBc staining (Fig. 6I). Specificity of human β2-microglobulin was confirmed by the absence of detection in mouse liver control tissue, with expression in chimeric human hepatocytes (Fig. 6I and Fig. S10). HBc staining showed successful infection in the human liver chimeric mice by different GTs; compared with GT A, B, C and E, more positive signals were found in GT D-infected human liver chimeric mice (Fig. 6J). To confirm the infectivity of the progeny virions of different GTs, mouse serum with high levels of viremia caused by GTs A, B, C and D, respectively, was used to infect HepG2-NTCP cells at a MOI of 50 (Fig. S11A). The successful infection was characterized by high level of HBV DNA 11 dpi and consistent with *in vitro* infection by HBVcc, the infectivity of GT D is higher than GT A ($p = 0.0091$), B ($p = 0.0188$) and C ($p = 0.0070$) (Fig. S11B). Infection of a naïve human liver chimeric mouse with serum from a viremic animal resulted in productive viremia (Fig. S11C, D). Taken together, these results firmly establish that our infectious clones of all genotypes form particles that are infectious in cell cultures and animals.

The constructed HBV clones are useful tools for clinical or preclinical drug assessment on different HBV genotypes

Since our HBV clones are constructed on a consistent vector backbone (pCRII-Blunt-TOPO) and HBV replication and viral protein expression are regulated under HBV endogenous enhancers and promoters, they are well suited for an unbiased assessment of the preclinical efficacy of anti-HBV therapeutics. Current standard of care is based on NAs, such as entecavir (ETV) and tenofovir, which act as HBV polymerase inhibitors.[37,38] However, even with long-term treatment, patients with CHB under NA monotherapy rarely achieve HBsAg loss (<5%) – an ideal endpoint for anti-HBV therapy and indicative of a functional cure.[37,39] More recently, core protein allosteric modulators (CpAMs) have been developed and their efficacy for treating CHB is currently being evaluated in clinical trials.

To establish proof-of-concept for the utility of the different HBV GTs for antiviral drug testing, the effects of CpAMs on different HBV GTs were tested. The analysis included both type I CpAMs, represented by GLS4 and Bay 41-419 which led to misassembled aberrant core polymers, and type II CpAMs (AT-130) which can induce HBV to form empty capsids with normal morphological characteristics but without viral nucleic acid.[40] Both experiments were conducted alongside ETV as a control (Fig. 7A). Treatment of HBV replicating cells with type I CpAMs GLS4 and Bay 41-419, other than type II CpAM AT-130, significantly suppressed HBsAg secretion for GTs A, B, D and E (Fig. 7B). In contrast to ETV, which had nearly no effect on HBeAg expression, all the CpAMs tested in this study efficiently inhibited HBeAg secretion for GTs A, B, D and E (Fig. 7C). Among different CpAMs, GLS4 showed the strongest HBeAg inhibition (by more than 50% across different GTs). Regarding inhibition of HBV replication ability, CpAMs did not demonstrate significant advantages over ETV in suppressing HBV DNA levels but GLS4 reduced HBV DNA levels more efficiently than ETV or Bay 41-419 and AT-130 for HBV GTs A, B and C (Fig. 7D). More importantly, CpAMs suppressed HBV pgRNA levels (>2 $\log_{10}$) 100- (GT C) to 1,000-fold (GTs A, B, D, E) (Fig. 7E). We then focused on GLS4 and tested the potential additive or synergistic effects of combining CpAM and NA treatment on suppressing our infectious clones. Increasing the concentration of GLS4 led to a dose-dependent HBeAg reduction for GTs A, B, D and E, but there were no obvious additive or synergistic effects caused by combining ETV and GLS4 on suppressing HBeAg and HBV DNA levels (Fig. 7F, Fig. S13A, C). For GTs B and E, there was stronger HBsAg inhibition with combined treatment than single drug treatment (Fig. 7F, Fig. S13B).

Finally, we aimed to corroborate these observations in an HBV infection system. To do so, HepG2-NTCP cells were infected with HBVcc of different GTs and subjected to treatment with GLS4 (Fig. 7G). In line with our data from the 1.3x HBV transfections, GLS4 administration results in suppression of HBeAg. Notably, suppression of HBeAg was most pronounced at later time points (11 dpi) while the treatment effects were minimal early on (Fig. 7H, Fig. S13D). More importantly, by 11 dpi, GLS4 treatment led to a significant reduction in both HBV DNA (Fig. 7I) and cccDNA (Fig. 7J) in the infected cells for all 5 GTs. For GTs A and D, about 80% of HBV DNA and cccDNA was reduced by GLS4 treatment compared to the mock treatment, which was even more pronounced than GTs B, C and E (Fig. S13E, F). Altogether, our data demonstrate that our constructed HBV clones are useful tools to assess the efficacy of clinical or preclinical drugs on different HBV GTs.

Discussion

In this study, we established and investigated HBV infectious clones of GTs A-E based on a consistent vector backbone and genome. While at least 9 HBV GTs have been described, HBV GTs A-E cover most HBV infections worldwide. Here, we assessed HBV replication, protein expression, infection capability, immune response, naturally occurring mutations, and clinical/preclinical drug sensitivity across different GTs *in vitro* and *in vivo* in immunodeficient and immunocompetent mice and human liver chimeric mice.

Cell lines such as HepG2.2.15[41] and HepAD38[42] that stably produce HBV have been commonly used for decades; however, they both produce HBV GT D (strain ayw). It is cumbersome to manipulate the integrated HBV genome in these cell lines to study the impact of specific mutations on HBV replication and/or virion assembly and release. Some HBV replication-competent plasmids of different GTs have been generated previously, but typically have only been used to investigate and compare HBV

transfected with the 1.3x HBV genomes and following 48 hours of ETV (250 nM) or GLS4 (250 nM, 500 nM, 1,000 nM) mono treatment or ETV (250 nM) and GLS4 (250 nM, 500 nM, 1,000 nM) combination. (G) Schematic showing the GLS4 (1 μM) administration in the *in vitro* infection system. (H) HBeAg levels at 5, 8, 11 days post infection with or without GLS4 (1 μM) treatment among different GTs. Quantification of intracellular HBV DNA (I) and HBV cccDNA (J) at 11 days post infection. LoD of the detection system ≈10^3 copies/ml. The data was shown as mean ± SD and at least 3 independent experiments were performed for each genotype. Unpaired 2-tailed *t* test. ***p* <0.01; ****p* <0.001; *****p* <0.0001. n.s., not significant. CLIA, chemiluminescence immunoassay; GT, genotype; LoD, limit of detection.

replication and protein expression *in vitro* across limited HBV strains which do not cover the major A-E genotypes.[26,27] Moreover, the infectivity of virions produced following transfection of such plasmids has hardly ever been included in the analysis across the different genotypes.

Another confounding problem hampering cross-comparisons is the inconsistency of HBV genome configurations including different lengths of the genomes, such as 1.05x,[43] 1.1x,[28] 1.2x,[44] 1.24x,[25] 1.28x[26] and 1.38x,[29] different vector backbones, and the use of either heterologous (CMV) promoters or endogenous HBV promoters and enhancers. Recently, Zhang *et al.* developed stable cell lines producing HBV virions of several different GTs[30]; however, their study used an ectopic CMV promoter to drive viral gene expression in stable cell lines, which may have interfered with regulation by endogenous HBV regulatory elements. Although these cell lines can still be useful, the titer of HBV from the stable cell lines is rather low ($\sim 10^6$ copies/ml) and thus large amounts of cell culture supernatant needed to be harvested and concentrated for the subsequent downstream infection assays. As with HepG2.2.15 and HepAD38, these stable cell lines are not suitable for HBV reverse genetic studies.

Since our infectious clones were constructed on a consistent pCRII-Blunt-TOPO cloning backbone, and HBV replication and viral protein expression are regulated under HBV endogenous enhancers and promoters, instead of an external CMV promoter, they are ideal models for parallel assessment of viral characteristics from different HBV GTs. By transfecting HepG2 cells with HBV-encoding plasmids, we found HBV DNA copy numbers were comparable across GTs A-E, while HBV pgRNA levels were 10-fold higher for GT C than the rest of the GTs. We also established proof-of-concept for utilizing our clones for preclinically evaluating the efficacy of CpAM and NA mono- or combination treatment in both transfection and infection systems. In the transfection model all 5 GTs significantly reduced markers of viral replication, confirming the pan-genotypic antiviral effects of CpAMs and NAs. In the infectious culture system, GT A and D were more sensitive to GLS4 treatment suggesting antiviral effects may also be related to the infectivity of different GTs. Notably, the GT C strain used in this study harbors mutations that may provide a selective advantage to the virus by increasing HBV replication capacity but reducing viral protein expression. Additional comparative studies including larger panels of GT C HBV – including strains that naturally express HBeAg – are needed to gain deeper insights into these apparent genotype-specific responses.

Previous work has revealed that HBV GTs exhibit different disease courses and respond differently to clinical treatment. Treatment with pegylated (peg)-IFN-α has been reported to be more effective in patients with CHB infected with GT A as characterized by HBeAg loss and a higher probability of HBsAg clearance than GTs B, C and D.[45,46] Another clinical study found that during the immune clearance phase, patients infected with GTs A and D were more likely to achieve an SVR than patients infected with GTs B, C and F, even under tenofovir monotherapy.[47] A recent study indicated that after NA withdrawal, patients infected with GTs A and D had higher HBsAg loss rates than other GTs.[48] Our experimental data are consistent with these clinical observations and may partially explain the underlying mechanisms for these differences. In immunocompetent C57BL/6 mice, we observed a more pronounced inflammatory response induced by HBV GTs A and D than GTs B, C and E, which was correlated with a more rapid decline in viral antigen and HBV DNA levels for these GTs.

In particular, multiple proinflammatory cytokines (IFN-γ, TNF-α, IL-6) and chemokines (CCL2 and CXCL10) were elevated in the sera of mice injected with GTs A and D compared with those injected with the other GTs. IFN signaling inhibits viral replication and modulates host immunity, while TNF-α can mediate anti-HBV immunity and induce liver inflammation. By analyzing patients with CHB, acute infection or patients experiencing flare-ups, Wang *et al.* found that TNF-α-producing HBV-specific CD4+ T cells might contribute to liver damage and HBV-specific IFN-γ-producing CD4 T cells were associated with HBV viral clearance.[49] The pleiotropic cytokine IL-6, secreted mainly by activated monocytes upon inflammatory stimulation, can contribute to the suppression of HBV infection but may augment pathogenesis by inflicting hepatocyte damage, and accelerating the development of cirrhosis and HCC.[50] This also partially explains why patients infected with HBV GT A are diagnosed with HCC ~6.5 years earlier than those infected with other GTs.[51] CCL2, also known as monocyte chemoattractant protein-1 or MCP-1, is implicated in the pathogenesis of diseases with monocytic infiltrates and is elevated during HBV infection.[52] CCL2 expression is negatively correlated with HBsAg levels and viral load.[53] The ligand of CXCR3, CXCL10, is an important immune chemoattractant during the IFN-induced inflammatory response and appears to be upregulated during HBV infection.[54] Notably, numerous studies have shown that CXCL10 can increase peripheral leukocyte migration to the liver, and that higher CXCL10 levels are associated with better treatment responses and even SVR in patients with CHB treated with NAs and peg-IFN.[55–57]

Interestingly, when we compare our original patient-derived HBV GT C with the one in which we rescued HBeAg expression, proinflammatory cytokines and chemokines increased *in vivo*. These findings are consistent with the notion that the patient-derived GT C strain evolved to gain a selective advantage. The most common mutations occur within the pre-core and core promoter regions and abolish or reduce the production of HBeAg. Patients with these HBV variants remain viremic and can develop progressive liver disease. It is conceivable that abrogating HBeAg expression – correlating in our strain with overall increased replicative fitness – together with reduced sensitivity to immune suppression, aids in establishing or maintaining viral persistence. Unfortunately, we do not have clinical information on the GT C serum donor and thus can only speculate about the impact on clinical outcome.

The differences that we observed in terms of liver pathology, immune responses or sensitivities to antiviral therapy can be conceivably attributed to genotype-specific features. Alternatively, some of the results could certainly be strain specific. Notably, we can exclude any differences based on variability in genome configuration and plasmid backbone as these were kept constant in the design of the 1.3x genomes. To discern these possibilities, larger panels of infectious clones will be needed for each of the GTs. Nonetheless, we could demonstrate our genetically defined infectious clones will be useful to reveal significant differences in inflammatory responses between viral GTs.

While the hydrodynamic delivery of the HBV genome-encoding plasmids offers a straightforward way to assess the replicative features and to characterize virally induced (immune-mediated) histopathology, only acute responses can be monitored. To establish a model of chronic *in vivo* infection, mouse livers can be transduced with adeno-associated virus (AAV) vectors carrying a replication-competent HBV DNA genome.[58–60] Previous studies have demonstrated that mice

injected with AAV-HBV can maintain HBV persistence for 6-50 weeks.[58–60] Our genetically tractable system will allow further study into the impact of viral (*e.g.* HBeAg) protein expression on pathogenesis and immunity using AAV-HBV strains on isogenic backgrounds.

Altogether, by constructing infectious clones of 5 HBV GTs and employing an *in vivo* study in immunocompetent mice, we found significant differences in inflammatory response among the different HBV GTs which are useful in unveiling the underlying molecular mechanisms for the different viral natural history, pathogenesis, disease progression and clinical treatment response among HBV GTs.

Abbreviations

AAV, adeno-associated virus; ALT, alanine aminotransferase; BCP, basic core promoter; cccDNA, covalently closed circular DNA; CHB, chronic hepatitis B; CpAM, core protein allosteric modulators; dpi, days post infection; DR, direct repeat; En, enhancer; ETV, entecavir; GT(s), genotype(s); HBV, hepatitis B virus; HBVcc, cell culture-derived HBV; HCC, hepatocellular carcinoma; HDI, hydrodynamic injection; IFN, interferon; IHC, immunohistochemistry; IL, interleukin; MOI, multiplicity of infection; NA, nucleos(t)ide analogue; NRG, NOD*Rag1*$^{-/-}$IL2RγNULL; PHH, primiary human hepatocyte; pgRNA, pre-genomic RNA; SVR, sustained virologic response.

Financial support

This study was funded in part by grants from the National Institutes of Health (R01AI138797 to L.S. and A.P.), (R01AI107301, R01AI146917, R01AI153236, R01AI168048 to A.P.) and (R01DK121072 all to R.E.S.), a Research Scholar Award from the American Cancer Society (RSG-15-048-01-MPC to A.P.), a Irma Hirschl Trust Research Scholar Award (R.E.S), a Burroughs Wellcome Fund Award for Investigators in Pathogenesis (101539 A.P.), and funds from Princeton University. This work also utilized an instrument acquired from a NIH SIG grants (S10OD026983 & S10OD030269 to N.A.C.).

Conflict of interest

The authors do not have any conflict of interest pertaining to this study. A.P. is president and founder of Acurasset Therapeutics, a consultant for PharmaSeq and Lycia Therapeutics, L.S. is founder of NPBioSciences, a consultant for Drugfarm and Neomics, and R.E.S. is on the scientific advisory board of Miromatrix Inc. and a speaker and consultant for Alnylam Inc.

Please refer to the accompanying ICMJE disclosure forms for further details.

Authors' contributions

The project was conceived and experiments designed by Y.L. and A.P. Experiments were performed by all authors. Data were analyzed by Y.L. A.T., N.A.C., R.E.S. and A.P. Critical reagents were provided by L.S. The manuscript was written by Y.L. and A.P with input from all authors.

Data availability statement

All data have been included in this manuscript. Sequence information have been deposited on NCBI as detailed in the supplementary Materials and Methods.

Acknowledgements

We thank Dr. Ju-Tao Guo (The Blumberg Institute) and Dr. Christoph Seeger (Fox Chase Cancer Center) for providing the rabbit anti-HBc polyclonal antibody and HepG2.2.15 cells, respectively. Dr. Peter Revill kindly provided a plasmid encoding the 1x HBV genotype B genome. We thank all members of the Ploss lab, in particular Drs. Lei Wei, Glenn Hogan, Emily Mesev and Robert LeDesma for critical discussion of the data and manuscript. This study was funded in part by grants from the National Institutes of Health R01AI138797 to L.S. and A.P.), (R01AI107301, R01AI146917, R01AI153236, R01AI168048 to A.P.) and (R01DK121072 to R.E.S.), a Research Scholar Award from the American Cancer Society (RSG-15-048-01-MPC to A.P.), an Irma Hirschl Trust Research Scholar Award (R.E.S), a Burroughs Wellcome Fund Award for Investigators in Pathogenesis (101539 A.P.), and funds from Princeton University. This work also utilized instruments acquired from NIH SIG grants (S10OD026983 & S10OD030269 to N.A.C.).

Supplementary data

Supplementary data to this article can be found online at https://doi.org/10.1016/j.jhepr.2022.100535.

References

Author names in bold designate shared co-first authorship

[1] Organization WH. Fact sheet, hepatitis B.. 2021 [cited 2021 December 2]; Available from: https://www.who.int/news-room/fact-sheets/detail/hepatitis-b.
[2] Park SG, Kim Y, Park E, Ryu HM, Jung G. Fidelity of hepatitis B virus polymerase. Eur J Biochem 2003;270:2929–2936.
[3] Kramvis A. Genotypes and genetic variability of hepatitis B virus. Intervirology 2014;57:141–150.
[4] Pourkarim MR, Amini-Bavil-Olyaee S, Kurbanov F, Van Ranst M, Tacke F. Molecular identification of hepatitis B virus genotypes/subgenotypes: revised classification hurdles and updated resolutions. World J Gastroenterol 2014;20:7152–7168.
[5] Tatematsu K, Tanaka Y, Kurbanov F, Sugauchi F, Mano S, Maeshiro T, et al. A genetic variant of hepatitis B virus divergent from known human and ape genotypes isolated from a Japanese patient and provisionally assigned to new genotype J. J Virol 2009;83:10538–10547.
[6] Locarnini S, Littlejohn M, Aziz MN, Yuen L. Possible origins and evolution of the hepatitis B virus (HBV). Semin Cancer Biol 2013;23:561–575.
[7] Kocher A, Papac L, Barquera R, Key FM, Spyrou MA, Hubler R, et al. Ten millennia of hepatitis B virus evolution. Science 2021;374:182–188.
[8] Norder H, Courouce AM, Coursaget P, Echevarria JM, Lee SD, Mushahwar IK, et al. Genetic diversity of hepatitis B virus strains derived worldwide: genotypes, subgenotypes, and HBsAg subtypes. Intervirology 2004;47:289–309.
[9] Velkov S, Ott JJ, Protzer U, Michler T. The global hepatitis B virus genotype distribution approximated from available genotyping data. Genes (Basel) 2018;9.
[10] Dupinay T, Restorp K, Leutscher P, Rousset D, Chemin I, Migliani R, et al. High prevalence of hepatitis B virus genotype E in Northern Madagascar indicates a West-African lineage. J Med Virol 2010;82:1515–1526.
[11] von Meltzer M, Vasquez S, Sun J, Wendt UC, May A, Gerlich WH, et al. A new clade of hepatitis B virus subgenotype F1 from Peru with unusual properties. Virus Genes 2008;37:225–230.
[12] Sunbul M. Hepatitis B virus genotypes: global distribution and clinical importance. World J Gastroenterol 2014;20:5427–5434.
[13] Lin CL, Kao JH. The clinical implications of hepatitis B virus genotype: recent advances. J Gastroenterol Hepatol 2011;26(Suppl 1):123–130.
[14] Suzuki Y, Kobayashi M, Ikeda K, Suzuki F, Arfase Y, Akuta N, et al. Persistence of acute infection with hepatitis B virus genotype A and treatment in Japan. J Med Virol 2005;76:33–39.
[15] Chan HL, Wong ML, Hui AY, Hung LC, Chan FK, Sung JJ. Hepatitis B virus genotype C takes a more aggressive disease course than hepatitis B virus genotype B in hepatitis B e antigen-positive patients. J Clin Microbiol 2003;41:1277–1279.
[16] Kao JH, Chen PJ, Lai MY, Chen DS. Hepatitis B genotypes correlate with clinical outcomes in patients with chronic hepatitis B. Gastroenterology 2000;118:554–559.
[17] Chan HL, Hui AY, Wong ML, Tse AM, Hung LC, Wong VW, et al. Genotype C hepatitis B virus infection is associated with an increased risk of hepatocellular carcinoma. Gut 2004;53:1494–1498.
[18] Yuen MF, Fung SK, Tanaka Y, Kato T, Mizokami M, Yuen JC, et al. Longitudinal study of hepatitis activity and viral replication before and after HBeAg seroconversion in chronic hepatitis B patients infected with genotypes B and C. J Clin Microbiol 2004;42:5036–5040.

[19] Xibing G, Xiaojuan Y, Juanhua W, Zhong H. Relationship between HBV genotypes B, C and follicular helper T cells in patients with chronic hepatitis B and its significance. Hepat Mon 2013;13:e6221.

[20] Raimondi S, Maisonneuve P, Bruno S, Mondelli MU. Is response to antiviral treatment influenced by hepatitis B virus genotype? J Hepatol 2010;52:441–449.

[21] Wai CT, Chu CJ, Hussain M, Lok AS. HBV genotype B is associated with better response to interferon therapy in HBeAg(+) chronic hepatitis than genotype C. Hepatology 2002;36:1425–1430.

[22] Erhardt A, Blondin D, Hauck K, Sagir A, Kohnle T, Heintges T, et al. Response to interferon alfa is hepatitis B virus genotype dependent: genotype A is more sensitive to interferon than genotype D. Gut 2005;54:1009–1013.

[23] Wiegand J, Hasenclever D, Tillmann HL. Should treatment of hepatitis B depend on hepatitis B virus genotypes? A hypothesis generated from an explorative analysis of published evidence. Antivir Ther 2008;13:211–220.

[24] Hsieh TH, Tseng TC, Liu CJ, Lai MY, Chen PJ, Hsieh HL, et al. Hepatitis B virus genotype B has an earlier emergence of lamivudine resistance than genotype C. Antivir Ther 2009;14:1157–1163.

[25] Sugiyama M, Tanaka Y, Kato T, Orito E, Ito K, Acharya SK, et al. Influence of hepatitis B virus genotypes on the intra- and extracellular expression of viral DNA and antigens. Hepatology 2006;44:915–924.

[26] Bhoola NH, Reumann K, Kew MC, Will H, Kramvis A. Construction of replication competent plasmids of hepatitis B virus subgenotypes A1, A2 and D3 with authentic endogenous promoters. J Virol Methods 2014;203:54–64.

[27] Sozzi V, Walsh R, Littlejohn M, Colledge D, Jackson K, Warner N, et al. In Vitro studies show that sequence variability contributes to marked variation in hepatitis B virus replication, protein expression, and function observed across genotypes. J Virol 2016;90:10054–10064.

[28] Li J, Li J, Chen S, Yuan Q, Zhang J, Wu J, et al. Naturally occurring 5' preS1 deletions markedly enhance replication and infectivity of HBV genotype B and genotype C. Gut 2021;70:575–584.

[29] Murayama A, Yamada N, Osaki Y, Shiina M, Aly HH, Iwamoto M, et al. N-terminal PreS1 sequence regulates efficient infection of cell-culture-generated hepatitis B virus. Hepatology 2021;73:520–532.

[30] **Zhang M**, **Zhang Z**, Imamura M, Osawa M, Teraoka Y, Piotrowski J, et al. Infection courses, virological features and IFN-alpha responses of HBV genotypes in cell culture and animal models. J Hepatol 2021;75:1335–1345.

[31] **Liu Y**, **Liu H**, **Hu Z**, **Ding Y**, Pan XB, Zou J, et al. Hepatitis B virus virions produced under nucleos(t)ide analogue treatment are mainly not infectious because of irreversible DNA chain termination. Hepatology 2020;71:463–476.

[32] **Wang J**, **Shen T**, **Huang X**, **Kumar GR**, Chen X, Zeng Z, et al. Serum hepatitis B virus RNA is encapsidated pregenome RNA that may be associated with persistence of viral infection and rebound. J Hepatol 2016;65:700–710.

[33] Pearson T, Shultz LD, Miller D, King M, Laning J, Fodor W, et al. Non-obese diabetic-recombination activating gene-1 (NOD-Rag1 null) interleukin (IL)-2 receptor common gamma chain (IL2r gamma null) null mice: a radioresistant model for human lymphohaematopoietic engraftment. Clin Exp Immunol 2008;154:270–284.

[34] Yang PL, Althage A, Chung J, Chisari FV. Hydrodynamic injection of viral DNA: a mouse model of acute hepatitis B virus infection. Proc Natl Acad Sci U S A 2002;99:13825–13830.

[35] Winer BY, Huang TS, Pludwinski E, Heller B, Wojcik F, Lipkowitz GE, et al. Long-term hepatitis B infection in a scalable hepatic co-culture system. Nat Commun 2017;8:125.

[36] MacPherson D, Bram Y, Park J, Schwartz RE. Peptide-based scaffolds for the culture and maintenance of primary human hepatocytes. Sci Rep 2021;11:6772.

[37] European Association for the Study of the Liver. Electronic address eee, European Association for the Study of the L. EASL 2017 Clinical Practice Guidelines on the management of hepatitis B virus infection. J Hepatol 2017;67:370–398.

[38] Terrault NA, Bzowej NH, Chang KM, Hwang JP, Jonas MM, Murad MH, et al. AASLD guidelines for treatment of chronic hepatitis B. Hepatology 2016;63:261–283.

[39] Liang TJ, Block TM, McMahon BJ, Ghany MG, Urban S, Guo JT, et al. Present and future therapies of hepatitis B: from discovery to cure. Hepatology 2015;62:1893–1908.

[40] Viswanathan U, Mani N, Hu Z, Ban H, Du Y, Hu J, et al. Targeting the multifunctional HBV core protein as a potential cure for chronic hepatitis B. Antivir Res 2020;182:104917.

[41] Sells MA, Chen ML, Acs G. Production of hepatitis B virus particles in Hep G2 cells transfected with cloned hepatitis B virus DNA. Proc Natl Acad Sci U S A 1987;84:1005–1009.

[42] Ladner SK, Otto MJ, Barker CS, Zaifert K, Wang GH, Guo JT, et al. Inducible expression of human hepatitis B virus (HBV) in stably transfected hepatoblastoma cells: a novel system for screening potential inhibitors of HBV replication. Antimicrob Agents Chemother 1997;41:1715–1720.

[43] **Yan H**, **Zhong G**, Xu G, He W, Jing Z, Gao Z, et al. Sodium taurocholate cotransporting polypeptide is a functional receptor for human hepatitis B and D virus. Elife 2012;1:e00049.

[44] **Wang J**, **Chen R**, **Zhang R**, Ding S, Zhang T, Yuan Q, et al. The gRNA-miRNA-gRNA ternary cassette combining CRISPR/Cas9 with RNAi approach strongly inhibits hepatitis B virus replication. Theranostics 2017;7:3090–3105.

[45] Flink HJ, van Zonneveld M, Hansen BE, de Man RA, Schalm SW, Janssen HL, et al. Treatment with Peg-interferon alpha-2b for HBeAg-positive chronic hepatitis B: HBsAg loss is associated with HBV genotype. Am J Gastroenterol 2006;101:297–303.

[46] **Buster EH**, **Hansen BE**, Lau GK, Piratvisuth T, Zeuzem S, Steyerberg EW, et al. Factors that predict response of patients with hepatitis B e antigen-positive chronic hepatitis B to peginterferon-alfa. Gastroenterology 2009;137:2002–2009.

[47] Marcellin P, Buti M, Krastev Z, de Man RA, Zeuzem S, Lou L, et al. Kinetics of hepatitis B surface antigen loss in patients with HBeAg-positive chronic hepatitis B treated with tenofovir disoproxil fumarate. J Hepatol 2014;61:1228–1237.

[48] **Sonneveld MJ**, **Chiu SM**, Park JY, Brakenhoff SM, Kaewdech A, Seto WK, et al. Probability of HBsAg loss after nucleo(s)tide analogue withdrawal depends on HBV genotype and viral antigen levels. J Hepatol 2022;76:1042–1050.

[49] **Wang H**, **Luo H**, **Wan X**, Fu X, Mao Q, Xiang X, et al. TNF-alpha/IFN-gamma profile of HBV-specific CD4 T cells is associated with liver damage and viral clearance in chronic HBV infection. J Hepatol 2020;72:45–56.

[50] **Chang TS**, **Wu YC**, Chi CC, Su WC, Chang PJ, Lee KF, et al. Activation of IL6/IGFIR confers poor prognosis of HBV-related hepatocellular carcinoma through induction of OCT4/NANOG expression. Clin Cancer Res 2015;21:201–210.

[51] Revill PA, Tu T, Netter HJ, Yuen LKW, Locarnini SA, Littlejohn M. The evolution and clinical impact of hepatitis B virus genome diversity. Nat Rev Gastroenterol Hepatol 2020;17:618–634.

[52] Fan Y, Wang L, Dou X. Serum monocyte chemoattractant protein-1 predicts liver inflammation of patients with chronic hepatitis B. Clin Lab 2018;64:841–846.

[53] Gunes H, Mete R, Aydin M, Topcu B, Oran M, Dogan M, et al. Relationship among MIF, MCP-1, viral loads, and HBs Ag levels in chronic hepatitis B patients. Turk J Med Sci 2015;45:634–637.

[54] Keating SM, Heitman JD, Wu S, Deng X, Stramer SL, Kuhns MC, et al. Cytokine and chemokine responses in the acute phase of hepatitis B virus replication in naive and previously vaccinated blood and plasma donors. J Infect Dis 2014;209:845–854.

[55] Zhou Y, Wang S, Ma JW, Lei Z, Zhu HF, Lei P, et al. Hepatitis B virus protein X-induced expression of the CXC chemokine IP-10 is mediated through activation of NF-kappaB and increases migration of leukocytes. J Biol Chem 2010;285:12159–12168.

[56] Yoshio S, Mano Y, Doi H, Shoji H, Shimagaki T, Sakamoto Y, et al. Cytokine and chemokine signatures associated with hepatitis B surface antigen loss in hepatitis B patients. JCI Insight 2018;3.

[57] **Guo R**, **Mao H**, Hu X, Zheng N, Yan D, He J, et al. Slow reduction of IP-10 Levels predicts HBeAg seroconversion in chronic hepatitis B patients with 5 years of entecavir treatment. Sci Rep 2016;6:37015.

[58] Dion S, Bourgine M, Godon O, Levillayer F, Michel ML. Adeno-associated virus-mediated gene transfer leads to persistent hepatitis B virus replication in mice expressing HLA-A2 and HLA-DR1 molecules. J Virol 2013;87:5554–5563.

[59] **Yang D**, **Liu L**, Zhu D, Peng H, Su L, Fu YX, et al. A mouse model for HBV immunotolerance and immunotherapy. Cell Mol Immunol 2014;11:71–78.

[60] **Ye L**, **Yu H**, Li C, Hirsch ML, Zhang L, Samulski RJ, et al. Adeno-associated virus vector mediated delivery of the HBV genome induces chronic hepatitis B virus infection and liver fibrosis in mice. PLoS One 2015;10:e0130052.